Proc. Natl. Acad. Sci. USA
Vol. 95, pp. 7145–7150, June 1998
Neurobiology

Neuronal coincidence detection by voltage-sensitive electrical synapses

DONALD H. EDWARDS*†, SHIH-RUNG YEH*, AND FRANKLIN B. KRASNE‡

*Department of Biology, Georgia State University, Atlanta, GA 30302-4010; and ‡Department of Psychology, University of California, Los Angeles, CA 90024

Communicated by Donald Kennedy, Stanford University, Stanford, CA, March 25, 1998 (received for review December 4, 1997)

ABSTRACT **Coincidence detection is important for functions as diverse as Hebbian learning, binaural localization, and visual attention. We show here that extremely precise coincidence detection is a natural consequence of the normal function of rectifying electrical synapses. Such synapses open to bidirectional current flow when presynaptic cells depolarize relative to their postsynaptic targets and remain open until well after completion of presynaptic spikes. When multiple input neurons fire simultaneously, the synaptic currents sum effectively and produce a large excitatory postsynaptic potential. However, when some inputs are delayed relative to the rest, their contributions are reduced because the early excitatory postsynaptic potential retards the opening of additional voltage-sensitive synapses, and the late synaptic currents are shunted by already opened junctions. These mechanisms account for the ability of the lateral giant neurons of crayfish to sum synchronous inputs, but not inputs separated by only 100 μsec. This coincidence detection enables crayfish to produce reflex escape responses only to very abrupt mechanical stimuli. In light of recent evidence that electrical synapses are common in the mammalian central nervous system, the mechanisms of coincidence detection described here may be widely used in many systems.**

Despite the importance of coincidence detection in many systems (1), including Hebbian learning (2–4), binaural localization (5–7), and visual attention (8, 9), the cellular mechanisms responsible for such detection are not well understood. Brevity of transmitter action, short postsynaptic membrane time constants, and rapidly activating outward currents that are triggered by excitatory postsynaptic potentials (EPSPs) can contribute to selective responsiveness to coincident stimuli (10–13). We report here that the properties of rectifying electrical synapses enable precise coincidence detection by a postsynaptic neuron that receives excitatory inputs from a converging array of these synapses. Coincidence detection is therefore an emergent property of rectifying synapses in a convergent network. Converging networks of this kind are realized in the afferent pathway to the lateral giant (LG) neuron of the crayfish, a command neuron for a tail flip escape reaction. We found that this network displays the predicted high degree of selection for coincident inputs.

METHODS

Theoretical. Each model neuron is a single electrical compartment with Hodgkin-Huxley conductances (14), and an electrical rectifier (Fig. 1*A*, diode symbol) with a voltage dependence similar to that of the giant motor synapse of crayfish (15, 16). For both model neurons, G_{NaMax} = 720 μS, G_{KMax} = 216 μS, G_L = 1 μS, E_{Na} = +45 mV (relative to a −70 mV rest potential), E_K = −82 mV, E_L = −60 mV, and C (compartmental capacitance) = 6 nF. These values are equivalent to those of the Hodgkin-Huxley model of the squid axon calculated for a temperature of 19°C and are not critical for the operation of the model. For the rectifying electrical synapses, the synaptic conductance is governed by the equation $G_j = G_{min} + (G_{max} - G_{min})/(1 + \exp(-A[V_{pre} - V_{post} - V_o]))$, where A = 0.15/mV, V_o = 70 mV, G_{max} = 20 μS, G_{min} = 0.2 μS, and V_{pre} and V_{post} are the voltages in the pre- and postsynaptic model neurons, respectively. This equation and all but one of these parameter values were taken directly from the description of voltage rectification at the giant motor synapse (15). The opening time constant for gap junctional conductance was assumed to be 0.2 ms, and the closing time constant was assumed to be 0.75 ms. These are within the range of published values for the temperature (19° − 20°C) at which the experiments were done (17). The slower closing time constant is not essential, but it does improve coincidence detection slightly. A more critical value is V_o, the value of the transynaptic potential at which the synaptic conductance is halfway between minimum and maximal values. This was set at 70 mV, 27 mV higher than the effective value of 43 mV measured at the giant motor synapse (15). With V_o = 70 mV, the summed EPSP evoked by two inputs was reduced by 16% when the delay between inputs was increased from 0 ms to 0.25 ms, and the peak inward current through the late synapse was reduced by 64% (Fig. 1*B*). When V_o = 43 mV, the EPSP was reduced by 10% and the current was reduced by 43% (not shown). The higher value of V_o will keep the synaptic conductance low until the presynaptic neuron is significantly depolarized. Any resting potential difference between the pre- and postsynaptic neurons will change the effective value of V_o; at the motor giant synapse, the presynaptic cell is 15 mV more negative than the postsynaptic cell.

For the nonrectifying electrical synapses, the synaptic conductance was fixed at 2.0 μS. For the excitatory chemical synapses, the reversal potential was 0 mV (relative to a resting potential of −70 mV), and the synaptic conductances each were governed by the equation $G_{syn} = G_{synmax}\,(t/\tau_s)^s\, e^{-(t/\tau s)}$, where G_{synmax} = 10 μS, s = 0.1, and τ_s = 0.1 ms.

Experimental. Juvenile crayfish (2–3 cm from rostrum to telson) that had been isolated for >1 month were chilled to immobility. The abdomen was removed and pinned out dorsal side up in a saline-filled Petri dish lined with Sylgard (Dow-Corning). The brain was mechanically destroyed. The fast extensor and fast flexor muscle was removed to expose the ventral nerve cord. Pairs of wire electrodes, insulated except at the tips, were placed on N2 and N3 of one side of the terminal ganglion, equidistant from the ganglion. A microelectrode (3 MKCl, 30 MΩ) was inserted through the ganglionic sheath into the proximal dendrite or initial axon segment of the projecting LG neuron. Shocks of 0.15 ms (from 5 to 10 V) were delivered

The publication costs of this article were defrayed in part by page charge payment. This article must therefore be hereby marked "*advertisement*" in accordance with 18 U.S.C. §1734 solely to indicate this fact.

Abbreviations: EPSP, excitatory postsynaptic potential; LG, lateral giant.

†To whom reprint requests should be addressed. e-mail: biodhe@panther.gsu.edu.

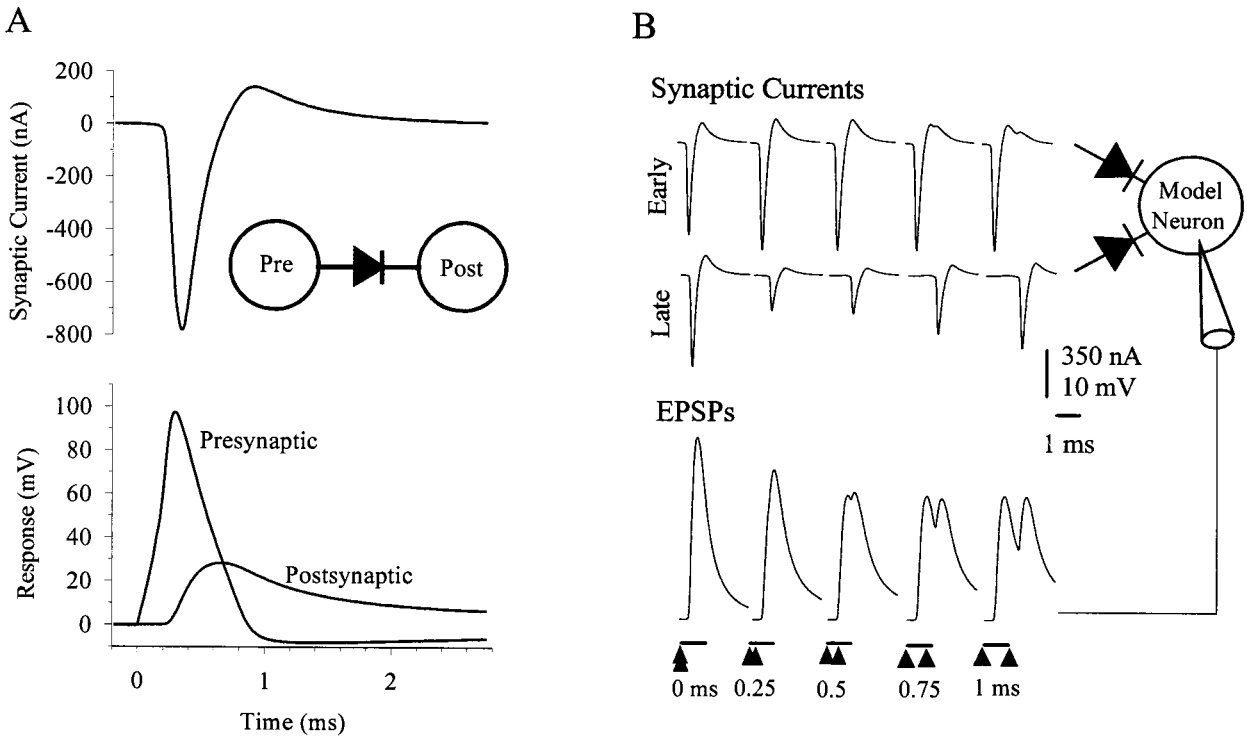

FIG. 1. Rectifying electrical synapses and coincidence detection in a model neuron. (*A*) Responses of a model rectifying electrical synapse. An action potential (*Lower*, Presynaptic) in a model presynaptic neuron (*Inset*, Pre ball) drives current (*Upper*) through the rectifying electrical synapse (*Inset*, black diode symbol), which produces an EPSP (*Lower*, Postsynaptic) in the model postsynaptic cell (*Inset*, Post ball). Note the delay in the onset of the EPSP and the reversal in synaptic current direction as the voltage across the synapse reverses. (*B*) Synaptic currents and EPSPs of a model neuron (circle in *Inset*) to coincident and asynchronous inputs through rectifying electrical synapses (diode symbols). The early synaptic currents (top traces at left) were evoked by presynaptic spikes identical to that in *A* through the top synapse (top diode symbol of *Inset*); the late synaptic currents (middle traces) were evoked by similar spikes presynaptic to the bottom synapse and delayed by the times given below the EPSPs. The EPSPs evoked by the early and late synaptic currents are at the bottom. The model was identical to that in *A*, except for the addition of a second synaptic input identical to the first.

to each nerve to evoke EPSPs in LG that were similar in amplitude (5–15 mV) and subthreshold when summed. Paired stimuli then were presented at 2-min intervals, in which the delay between the stimuli in each pair varied from +5 ms to −5 ms in a random sequence. EPSP amplitudes following the second stimulus were measured off-line. The maximal EPSP amplitude (usually the β wave) was measured as the peak depolarization. The α EPSP was measured as the first depolarizing peak; it occurred within 0.1–0.3 ms of the second stimulus. Responses at each delay were averaged and then normalized to the maximal response. The normalized responses at each delay were averaged across the preparations in each experiment.

RESULTS

Rectifying electrical synapses are found in both invertebrates (18–20) and vertebrates (21, 22), where they mediate unidirectional electrical coupling between neurons. In invertebrates (23), rectification appears to be mediated by pre- and postsynaptic connexin-like proteins that are sensitive to junctional potential (24, 25). To determine the consequences of rectifying electrical synapses on coincidence detection, we modeled each of these synapses as a voltage-sensitive conductance that linked a presynaptic action potential to a single-compartment postsynaptic model neuron (Fig. 1*A*). Rectifying electrical synapses provide a high-conductance pathway between pre- and postsynaptic neurons when the synapse is polarized with the presynaptic side more positive than the postsynaptic side. A presynaptic spike will drive current through the rectifying synapse as the transynaptic conductance increases, and so produce an EPSP (Fig. 1*A*). The polarization of the synapse will reverse as the presynaptic cell repolarizes and the postsynaptic cell reaches the peak of its EPSP. Although the transynaptic conductance may begin to decrease, the relatively high conductance level persists for some time and enables current to be driven out of the now reverse-polarized synapse. This outward current shortens the duration of the EPSP.

Coincidence detection can occur when two or more inputs converge on a postsynaptic neuron through rectifying electrical synapses, as in the model of Fig. 1*B*. If the inputs are synchronous, the inward currents sum, and the EPSP rises faster and to a higher level (Fig. 1*B*, first column of responses) than with a single input (Fig. 1*A*). When inputs are slightly asynchronous (e.g., a delay of 250 μs), the EPSP created by the first input greatly reduces the effect of the second input (Fig. 1*B*, second column of responses). The early EPSP created by the first input creates a reverse polarization of the second synapse, and so delays the transition of that synapse from low to high conductance on arrival of the delayed presynaptic spike. The EPSP also reduces the driving force on the inward current through the late synapse. These two mechanisms greatly reduce the inward current entering through the delayed synapse (Fig. 1*B*, middle trace of the second column). In addition, the initial outward current creates a shunt for the inward current from the second input; the effect of this mechanism is apparent in the slight increase in the outward current through the early synapse (Fig. 1*B*, top trace of second column). Together these effects cause the delayed EPSP to reach a peak amplitude well below that achieved by coincident inputs (Fig. 1*B*, bottom trace in second column).

With larger delays, the inhibitory effect of the first input on the second is reduced, and so the early and delayed EPSPs sum more linearly (Fig. 1*B*, third and later columns of traces).

However, the outward current at the first synapse reduces the initial EPSP quickly after the peak, and so prevents later EPSPs from summing with the peak of the early EPSP.

The discrimination against late inputs does not occur if the synapses are nonrectifying electrical synapses, or if they are chemical excitatory synapses with a common reversal potential (Fig. 2). In the first case, the inputs are nearly additive because the system is nearly linear. This is apparent in Fig. 2*A*, where responses of the same postsynaptic model neuron were calculated for coincident and asynchronous inputs. The inputs are produced by action potentials in two presynaptic neurons (not shown) that are each linked to the postsynaptic model cell by a 0.5 MΩ synaptic resistance. Neither the synaptic currents nor the summed EPSPs are greatly affected by the delay in the two inputs. In the case of chemical synaptic inputs, the early and late synaptic conductances can be regarded as one pulsatile postsynaptic conductance that charges the cell toward a common reversal potential. This is apparent in Fig. 2*B*, where responses of the same postsynaptic model neuron are shown for coincident and asynchronous changes in postsynaptic conductance. The summed EPSPs are not affected by the delay between synaptic inputs. The decay of the summed response is much slower than in the previous two examples because it is governed entirely by the membrane time constant, rather than by shunts created by the electrical synapses. Finally, it should be noted that the coincidence detection ability of all three mechanisms can be improved by reducing the duration of the EPSP, either by enabling the synaptic current to be drawn off into other parts of the postsynaptic neuron, or by reducing the membrane time constant of the postsynaptic cell. These changes will still leave the first mechanism, with the rectifying electrical synapses, as the most effective means of coincidence detection.

Massively convergent excitation of high-threshold giant neurons plays an important role in triggering the short-latency tail flip escape responses of the crayfish (26–30). An attack on the rear of the animal will excite many mechanosensory afferents, including both surface hair cells and hinge stretch receptors in the tail fan. These afferents converge directly on the LG interneuron and excite mechanosensory interneurons that also converge on the LG neuron (Fig. 3*A*) (31, 32). The LG neuron fires if the stimuli are abrupt; slowly increasing mechanosensory stimuli (e.g., a gradually increasing pinch of the tail fan) fail to excite LG but instead excite a longer latency, less stereotyped form of tail flip that is mediated by nongiant interneurons (33). Some selectivity of the LG neuron for phasic inputs would be expected from feed-forward inhibition (34) and lateral inhibition (35) that curtail LG's EPSP. However, because the synapses made by both primary afferents and interneurons on the LG neurons are electrical rectifiers (32, 36, 37), we also expected that the mechanism described above might contribute to coincidence detection. Moreover, coincidence detection based on voltage-sensitive electrical transmission would be expected to be extremely precise, operating on a submillisecond time scale, whereas feed-forward and recurrent inhibition require several msec for their onset. This expectation led us to investigate the possibility of high-precision coincidence detection by the LG neurons.

We tested for coincidence detection by comparing the LG neuron's responses to inputs from two sensory nerves evoked by stimuli that were separated by a variable short delay (see *Methods*). When stimulation of nerve 3 (N3) of the terminal ganglion (A6, Fig. 3*A*) of a juvenile (2 cm) crayfish occurred 100 μs before stimulation of N2, a large, rapidly rising EPSP was evoked in the LG neuron (Fig. 3*B*). When the delay was increased or decreased by 100 μs the response fell by between 30% and 50% (averages of −28% and −35%, respectively). A slight difference in the placement of the stimulus electrodes along the length of the two nerves may account for the offset of the response peak from zero delay.

Sharp coincidence effects have been seen in five other preparations, where the response fell symmetrically by 20% at 100 μs on either side of the peak. In a total of 18 preparations, the average of their normalized peak responses was less

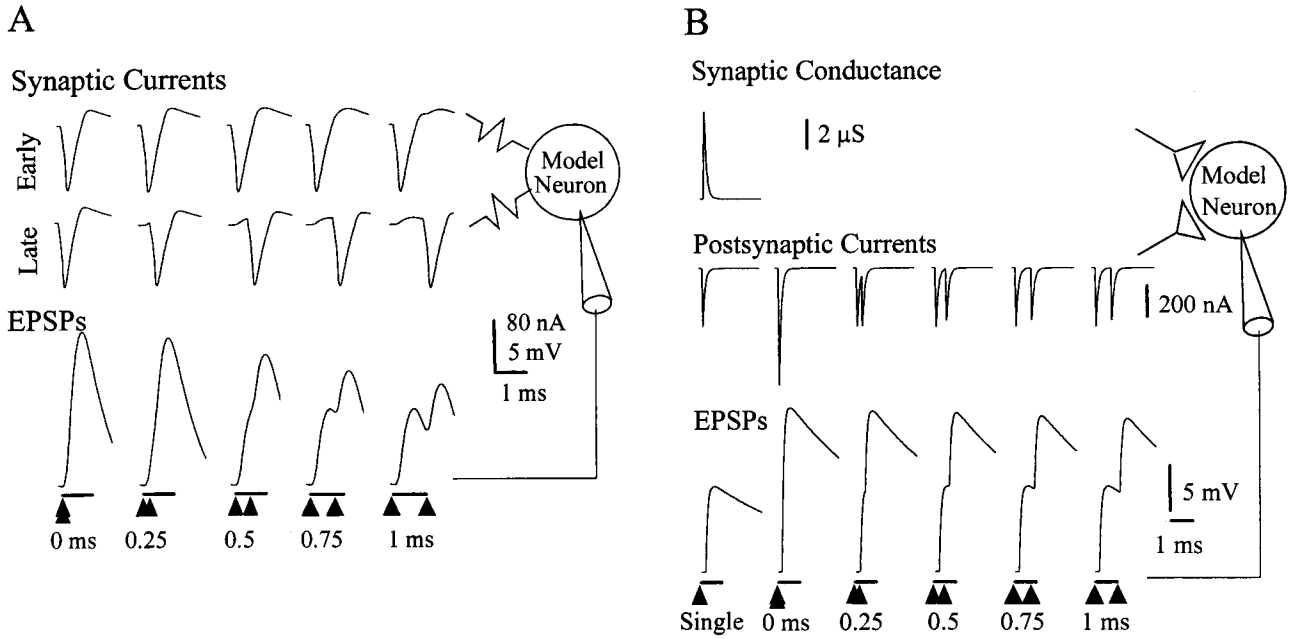

FIG. 2. Postsynaptic responses of the same model neuron to coincident and asynchronous inputs through nonrectifying electrical synapses and chemical synapses. (*A*) Nonrectifying electrical synapses (resistance symbols in *Inset*). The early synaptic currents (top traces at left) were evoked by presynaptic spikes identical to that in Fig. 1*A* through the top synapse (top resistance symbol of *Inset*); the late synaptic currents (middle traces) were evoked by similar spikes presynaptic to the bottom synapse and delayed by the times given at the bottom. The EPSPs evoked by those currents are given below. The model was identical to that in Fig. 1*B*, except that ohmic resistances (1 MΩ) were substituted for the rectifying electrical synapses. (*B*) Chemical synapses (triangular symbols in *Inset*) were implemented by time-varying conductances (*Top*) in series with 0 mV reversal potentials (relative to a rest potential of −70 mV). Postsynaptic currents (*Middle*) and EPSPs (*Bottom*) were calculated for a single synaptic input, for a pair of coincident inputs, and for pairs of staggered inputs delayed by the times given below.

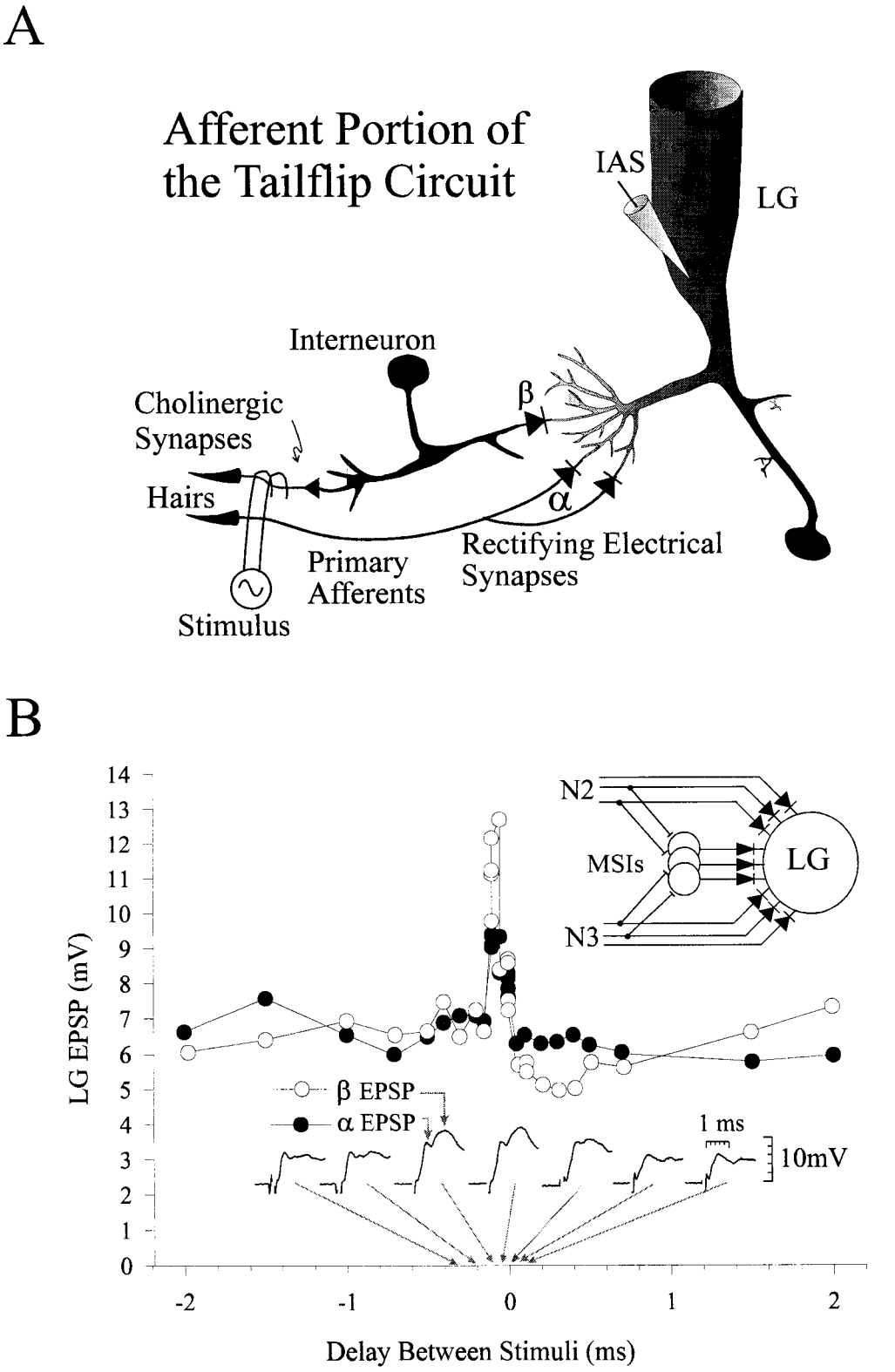

FIG. 3. Coincidence detection in the crayfish escape circuit. (*A*) The tail flip circuit in crayfish, showing convergence of mechanosensory afferents and interneurons (MSIs) on LG. Hairs and other mechanoreceptors on the abdominal surface project primary afferents through several sensory nerves into the central nervous system where they excite the LG neuron directly (α) and indirectly through mechanosensory interneurons (β). All LG neuron inputs are mediated through rectifying electrical synapses (diode symbols). EPSPs were recorded in the initial axon segment (IAS) of the LG neuron. The circuit was activated experimentally by brief shocks applied to pairs of sensory nerves (stimulus). (*B*) Coincidence detection at LG. The amplitudes of the α and β components of the LG EPSP are plotted against the delay between shocks of sensory nerves 2 (N2) and 3 (N3). Primary afferents from these nerves evoke the α EPSP, and interneurons excited by those same afferents evoke the β EPSP (see *Inset*). Traces of the recorded compound EPSPs evoked by coincident or noncoincident shocks delivered to N2 and N3 of the terminal ganglion are presented below the graph. The delay between stimuli in each pair is given by the arrows; positive values correspond to presentation of the N2 stimulus before the N3 stimulus. α and β EPSP peaks (arrows) were identified in each trace, respectively, as the first and second waves of depolarization and were measured and plotted separately against the delay between stimuli.

dramatic but still significant: the asynchronous response was reduced by 14% ± 2.5% (SEM) if the delay between synaptic inputs was 0.1 ms (Fig. 4*A*).

Both monosynaptic and disynaptic inputs contribute to the LG EPSP evoked by sensory nerve stimulation. Two methods were used to separate the contributions to coincidence detection of the two pathways to the LG neuron. In some experiments the monosynaptic response was isolated by reducing the stimulus amplitude to below the level needed to excite the mechanosensory interneurons (MSIs) (Fig. 4*B*). In others (not shown), excitation of the MSIs was prevented by superfusing the preparation with 50 μM mecamylamine, which blocks nicotinic transmission from primary afferents to MSIs (34). In both cases the alpha component was largest when the two nerves were stimulated simultaneously and declined with increasing delay between them. This result (Fig. 4*B*) was essentially the same as that obtained when both monosynaptic and disynaptic pathways to LG were operative (Fig. 4*A*).

It seemed unlikely that feed-forward inhibition, which reduces EPSPs produced by a second stimulus that follows a first by several msec, could account for the results observed here (34); however, it seemed necessary to verify this. Feed-forward inhibition is mediated by γ-aminobutyric acid and is known to be sensitive to picrotoxin, which enhances the β EPSP (36, 38).

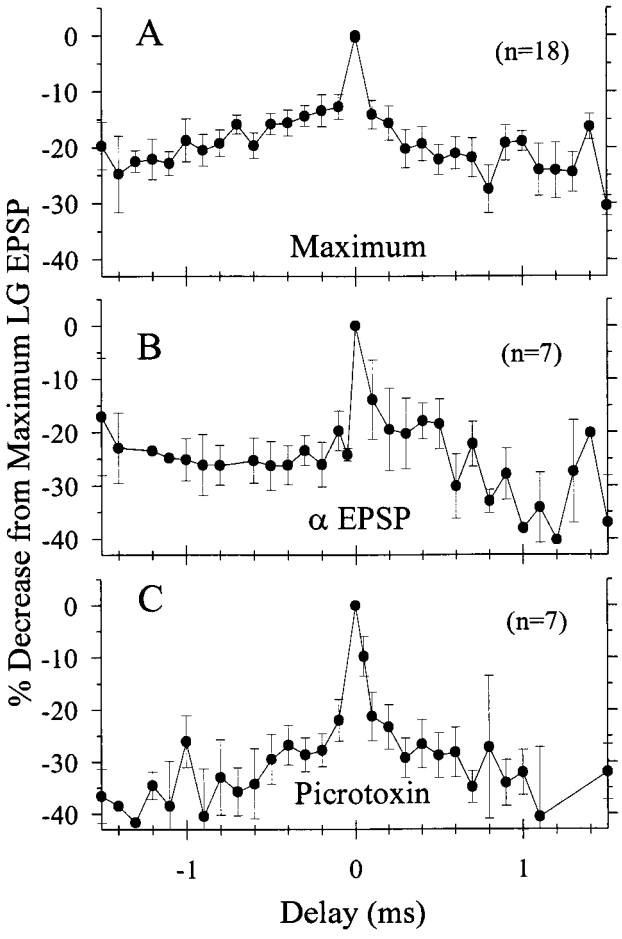

FIG. 4. Coincidence detection by the LG neuron. The normalized average EPSPs evoked in the LG neuron by pairs of coincident and noncoincident electrical stimuli to nerves 2 (N2) and 3 (N3) of the terminal ganglion are plotted against the time delay between stimuli in each pair. (*A*) Maximal depolarization in each EPSP (α or β component). (*B*) α EPSP evoked by reducing the stimulus strengths to levels below threshold for exciting mechanosensory interneurons that contribute to the β EPSP in the LG neuron. (*C*) Maximal EPSP recorded during superfusion of the nerve cord with 10 μM picrotoxin.

We found the sensitivity of LG to coincident stimuli was, if anything, sharper in the presence of picrotoxin than without it. Delays of 50 μs between stimuli caused the summed response to decrease by 10% from the coincident value, and delays of more than 100 μs reduced the response by 20% (Fig. 4*C*).

DISCUSSION

The sensitivity to coincident input predicted for converging rectifying electrical synapses is confirmed for the LG circuit. A factor partially responsible for the predicted sensitivity to coincidence is that current that otherwise would contribute to generating an EPSP is shunted into afferent terminals of those junctions that have been previously activated by a presynaptic spike. Consistent with this, we have found that a spike in an afferent terminal enables a later LG EPSP to be recorded in the terminal; the antidromic synaptic potential is not seen in the terminal without the earlier afferent spike (not shown).

These theoretical and experimental results have identified an additional role for rectifying electrical synapses, that of mediating coincidence detection in networks of convergent neurons. This role emerges from the properties of the synapses that cause each presynaptic action potential to evoke a biphasic flow of synaptic current; a phasic current into the postsynaptic cell is immediately followed by a smaller current out of the cell that curtails the EPSP. This same succession of inward and outward postsynaptic currents underlies coincidence detection that mediates binaural localization in birds, where a chemical EPSP in neurons of the nucleus laminaris immediately evokes an outward membrane current produced by a rapidly activating potassium conductance (11, 12). As in the present case, this voltage-activated outward current serves to curtail the EPSP and to discriminate against summation of late synaptic inputs. We propose that the rapid succession of postsynaptic inward and outward currents is necessary at both types of synapses to minimize the period of effective spatial summation of distinct synaptic inputs, and so to mediate precise coincidence detection at single neurons. We also propose that this mechanism for coincidence detection is most effective when the inputs are only a short electrical distance apart. The phasic nature of the EPSP from one input site will be lost as it spreads to a second, electrically distant, input site, as will the shunting effect of one input on the other. As a result, synaptic coincidence detection that is mediated by the flow and ebb of synaptic currents is likely to operate locally, within a single dendrite or region of the postsynaptic neuron.

It is not known whether rectifying electrical synapses contribute to coincidence detection in other animals. However, the presence of electrical synapses in the nervous systems of invertebrates (18–20), and the high frequency of mixed excitatory synapses in the spinal cord of rats (between 30% and 100% of all excitatory synapses) (39), suggests that this simple mechanism for coincidence detection by single neurons may be in broad use across animal phyla.

We thank Drs. William Heitler, Paul S. Katz, and Ulrike Spörhase-Eichmann for their many helpful comments. This work was supported by the U.S. National Science Foundation.

1. Konnerth, A., Tsien, R. Y., Mikoshiba, K. & Altman, J. (1996) *Coincidence Detection in the Nervous System* (Human Frontier Science Program, Strasbourg, France).
2. Hebb, D. O. (1949) *The Organization of Behavior: A Neuropsychological Theory* (Wiley, New York).
3. Brown, T. H., Kairiss, E. W. & Keenan, C. L. (1990) *Annu. Rev. Neurosci.* **13,** 475–511.
4. Harris, E. W., Ganong, A. H. & Cotman, C. W. (1984) *Brain Res.* **323,** 132–137.
5. Boudreau, R. E. & Carr, C. E. (1993) *Brain Res.* **628,** 330–334.
6. Pena, J. L., Viete, S., Albeck, Y. & Konishi, M. (1996) *J. Neurosci.* **16,** 7046–7054.

7. Hoy, R., Nolen, T. & Brodfuehrer, P. (1989) *J. Exp. Biol.* **146,** 287–306.
8. Kreiter, A. K. & Singer, W. (1996) *J. Neurosci.* **16,** 2381–2396.
9. Singer, W. & Gray, C. M. (1995) *Annu. Rev. Neurosci.* **18,** 555–586.
10. Konig, P., Engel, A. K. & Singer, W. (1996) *Trends Neurosci.* **19,** 130–137.
11. Reyes, A. D., Rubel, E. W. & Spain, W. J. (1996) *J. Neurosci.* **16,** 993–1007.
12. Reyes, A. D., Rubel, E. W. & Spain, W. J. (1994) *J. Neurosci.* **14,** 5352–5364.
13. Manis, P. B. & Marx, S. O. (1991) *J. Neurosci.* **11,** 2865–2880.
14. Hodgkin, A. L. & Huxley, A. F. (1952) *J. Physiol. (London)* **117,** 500–544.
15. Giaume, C., Kado, R. T. & Korn, H. (1987) *J. Physiol. (London)* **386,** 91–112.
16. Furshpan, E. J. & Potter, D. D. (1959) *J. Physiol. (London)* **145,** 289–325.
17. Jaslove, S. W. & Brink, P. R. (1986) *Nature (London)* **323,** 63–65.
18. Nichols, J. G. & Purves, D. (1972) *J. Physiol. (London)* **225,** 637–656.
19. Heitler, W. J., Fraser, K. & Edwards, D. H. (1991) *J. Comp. Physiol. A* **169,** 707–718.
20. Spira, M. E. & Bennett, M. V. L. (1971) *Brain Res.* **37,** 294–300.
21. Auerbach, A. A. & Bennett, M. V. L. (1969) *J. Gen. Physiol.* **53,** 211–237.
22. Gilat, E., Hall, D. H. & Bennett, M. V. (1986) *Brain Res.* **365,** 96–104.
23. Barnes, T. M. (1994) *Trends Genet.* **10,** 303–305.
24. Phelan, P., Stebbings, L. A., Baines, R. A., Bacon, J. P., Davies, J. A. & Ford, C. (1998) *Nature (London)* **391,** 181–184.
25. Bennett, M. V. (1997) *J. Neurocytol.* **26,** 349–366.
26. Wiersma, C. A. G. (1947) *J. Neurophysiol.* **10,** 23–38.
27. Wine, J. J. & Krasne, F. B. (1982) in *The Cellular Organization of Crayfish Escape Behavior*, eds. Sandeman, D. C. & Atwood, H. L. (Academic, New York), pp. 241–292.
28. Olson, G. C. & Krasne, F. B. (1981) *Brain Res.* **214,** 89–100.
29. Krasne, F. B. (1969) *J. Exp. Biol.* **50,** 29–46.
30. Kennedy, D., Zucker, R. S. & Selverston, A. I. (1971) *Science* **173,** 645–650.
31. Newland, P. L., Aonuma, H. & Nagayama, T. (1997) *J. Comp. Physiol. A* **181,** 103–109.
32. Zucker, R. S. (1972) *J. Neurophysiol.* **35,** 599–618.
33. Wine, J. J. & Krasne, F. B. (1972) *J. Exp. Biol.* **56,** 1–18.
34. Vu, E. T., Berkowitz, A. & Krasne, F. B. (1997) *J. Neurosci.* **17,** 8867–8879.
35. Kennedy, D., Calabrese, R. L., Wine, J. J. & Calabrese, R. (1974) *Science* **186,** 451–454.
36. Edwards, D. H., Heitler, W. J., Leise, E. M. & Fricke, R. A. (1991) *J. Neurosci.* **11,** 2117–2129.
37. Lee, S. C. & Krasne, F. B. (1993) *J. Comp. Neurol.* **327,** 271–288.
38. Vu, E. T. & Krasne, F. B. (1993) *J. Neurosci.* **13,** 4394–4402.
39. Rash, J. E., Dillman, R. K., Bilhartz, B. L., Duffy, H. S., Whalen, L. R. & Yasumura, T. (1996) *Proc. Natl. Acad. Sci. USA* **93,** 4235–4239.